UC Davis
UC Davis Previously Published Works

Title

Inactivation of Medial Frontal Cortex Changes Risk Preference.

Permalink

https://escholarship.org/uc/item/7gd463sj

Journal

Current Biology, 28(19)

Authors

Stuphorn, Veit
Chen, Xiaomo

Publication Date

2018-10-08

DOI

10.1016/j.cub.2018.07.043

Copyright Information

This work is made available under the terms of a Creative Commons Attribution-NonCommercial-NoDerivatives License, available at https://creativecommons.org/licenses/by-nc-nd/4.0/

Peer reviewed

eScholarship.org Powered by the California Digital Library
University of California

Author Manuscript

Author Manuscript

Author Manuscript

Author Manuscript

HHS Public Access

Author manuscript

Curr Biol. Author manuscript; available in PMC 2019 October 08.

Published in final edited form as:

Curr Biol. 2018 October 08; 28(19): 3114–3122.e4. doi:10.1016/j.cub.2018.07.043.

Inactivation of medial frontal cortex changes risk preference

Xiaomo Chen[1,2,3] and **Veit Stuphorn***[1,2]

[1]Department of Neuroscience, Johns Hopkins University School of Medicine and Zanvyl Krieger Mind/Brain Institute, 3400 N. Charles St., Baltimore, MD 21218-2685, USA

[2]Department of Psychological and Brain Sciences, Johns Hopkins University, 3400 N. Charles St., Baltimore, MD 21218-2685, USA

Summary

Humans and other animals need to make decisions under varying degrees of uncertainty. These decisions are strongly influenced by an individual's risk preference, however the neuronal circuitry by which risk preference shapes choice is still unclear [1]. Supplementary eye field (SEF), an oculomotor area within primate medial frontal cortex, is thought to be an essential part of the neuronal circuit underlying oculomotor decision-making, including decisions under risk [2–5]. Consistent with this view, risk-related action value and monitoring signals have been observed in SEF [6–8]. However, such activity has also been observed in other frontal areas, including orbitofrontal [9–11], cingulate [12–14], and dorsal lateral frontal cortex [15]. It is thus unknown whether the activity in SEF causally contributes to risky decisions, or if it is merely a reflection of neural processes in other cortical regions. Here, we tested a causal role of SEF in risky oculomotor choices. We found that SEF inactivation strongly reduced the frequency of risky choices. This reduction was largely due to a reduced attraction to reward uncertainty and high reward gain, but not due to changes in the subjective estimation of reward probability or average expected reward. Moreover, SEF inactivation also led to increased sensitivity to differences between expected and actual reward during free choice. Nevertheless, it did not affect adjustments of decisions based on reward history.

eTOC Blurb

Corresponding author and lead contact: Veit Stuphorn, Johns Hopkins University, 338 Krieger Hall, 3400 N. Charles St., Baltimore, MD 21218, USA, Tel: (410) 516-7964, Fax: (410) 516-8648, veit@jhu.edu.

[3]Current address: Department of Neurobiology, Stanford University School of Medicine, Stanford University, Clark Center W1.3, 318 Campus Drive West Stanford, CA 94305

Author contributions

X.C. and V.S. formulated the hypotheses, designed the experiment, analyzed the data, and drafted the manuscript; V.S. secured funding; X.C. carried out the experiment and collected the data.

Publisher's Disclaimer: This is a PDF file of an unedited manuscript that has been accepted for publication. As a service to our customers we are providing this early version of the manuscript. The manuscript will undergo copyediting, typesetting, and review of the resulting proof before it is published in its final citable form. Please note that during the production process errors may be discovered which could affect the content, and all legal disclaimers that apply to the journal pertain.

Declaration of interests

The authors declare no competing interests

DATA AND SOFTWARE AVAILABILITY

Data and software are available upon request to the Lead Contact (veit@jhu.com).

Author Manuscript

Author Manuscript

Author Manuscript

Author Manuscript

Chen et al. (2018) report a causal role of medial frontal cortex in regulating risky and impulsive behavior in risky decisions. These findings provide new insight into the neuronal circuits underlying inconsistent, context dependent choices under risk observed across humans and non-human primates.

Results

Monkeys are risk-seeking

In our gambling task, two monkeys (*Macaca mulatta*, A and I) had to choose between two gambles with different combinations of maximum reward amount and winning probability (Figure 1A and Methods). Risk was quantified as reward uncertainty, using standard economic models [16–18].

The monkeys used the gamble cues in an economically rational way. They consistently selected gambles with higher reward amount (error rates: Monkey A: 9.22%; Monkey I: 1.99%; Figure 2A) and higher winning probability (error rates: Monkey A: 4.94%; Monkey I: 2.75%; Figure 2A) when the other attribute was matched. Overall, the monkeys clearly preferred options with higher expected value (EV) (Figure S1 A, B, H, and I). The monkeys were also risk-seeking, consistent with many previous studies [6,10,19,20]. For gambles with identical EV, both monkeys preferred the gamble option with the higher outcome variance, i.e. higher risk (Figure 2B, t-test, Monkey A: P(choose more risky option)=79.01%, t-test: p=2.37×10^{-6}; Monkey I: P(choose more risky option)=73.40%, t-test: p=5.19×10^{-4}).

We quantified the monkeys' risk preference using two standard economic models: the risk-value and the prospect theory model (Methods). The risk-value model is derived from financial theory and decomposes the subjective value of each option into a weighted linear combination of EV and variance risk, computed as the variance (Var) of the gamble outcomes [10,16,17]. It outperformed models using only the EV or the Var term, and models using coefficient of variance of the gamble outcomes, an alternative measure of risk [22] (Table S2). The monkeys preferred options with higher EV (Figure 2C, t-test, Monkey A: $\overline{\beta_{EV}}$ = 5.08, p= 5.60×10^{-8}; Monkey I: $\overline{\beta_{EV}}$ = 6.39, p= 8.03×10^{-11}) and higher Var, leading to risk seeking behavior, (Figure 2C, t-test, Monkey A: $\overline{\beta_{Var}}$ = 4.29, p= 2.03×10^{-6}; Monkey I: $\overline{\beta_{Var}}$ = 2.60, p= 7.00×10^{-5}).

The prospect theory model is derived from expected utility theory and estimates subjective value using a non-linear utility and probability weighting function [9,22,23]. This model predicted the monkeys' choice behavior better than models using either utility or probability weighting functions alone, and also slightly better than the risk-value model (Table S2). The best-fitting utility functions of both monkeys were convex (Figure 2 D and E, t-test, Monkey A: $\overline{\rho}$ = 1.47, $H1$:$\overline{\rho} \neq 1$, p= 2.39×10^{-11}; Monkey I: $\overline{\rho}$ = 1.42, $H1$: $\overline{\rho} \neq 1$, p= 6.30×10^{-12}). In addition, the monkeys also significantly overweighed low and underweighted high probabilities (Figure 2 E and F, t-test, Monkey A: $\overline{\alpha}$= 0.65, $H1$: $\overline{\alpha} \neq 1$, p= 2.32×10^{-10}; Monkey I: $\overline{\alpha}$= 0.86, $H1$: $\overline{\alpha} \neq 1$, p= 0.03). Therefore, the monkeys were attracted

Author Manuscript

Author Manuscript

Author Manuscript

Author Manuscript

disproportionally to large reward amounts and overestimated the likelihood of obtaining them when the winning probability was low, leading to risk seeking behavior.

Thus, both economic models indicated a strong preference for riskier options. In contrast, there was only very weak evidence for directional bias (risk-value model: t-test, Combined: $\overline{\beta_d}$ = 0.06, p=0.21; Monkey A: $\overline{\beta_d}$ = 0.04, p=0.23; Monkey I: $\overline{\beta_d}$ = 0.07, p=0.42; prospect theory model: t-test, Combined: d = 0.06, p=0.01; Monkey A: $\overline{d}$= 0.04, p=0.05; Monkey I: $\overline{d}$ = 0.09, p=0.03). There was no evidence that the monkeys tended to repeat the previous choice direction (t-test, Combined: $\overline{\beta_d}$ = 0.06, p=0.21; Monkey A: $\overline{\beta_d}$ = 0.04, p=0.23; Monkey I: = 0.07, p=0.42).

SEF inactivation reduces risk-seeking

SEF neurons encode action value signals that reflect the subjective value of options in the oculomotor gambling task and are correlated with the monkeys' choices [8]. To test if these signals have a causal effect on decision making, we examined whether bilateral inactivation of SEF influenced monkeys' behavior in the oculomotor gambling task, using a cryoplate (Figure 1 C and D). This method allows us to quickly and reversibly inactivate the SEF in both hemispheres [24]. We monitored neuronal activity in both SEF hemispheres during control and inactivation conditions. Consistent with previous reports [25,26], the spiking activity decreased with decreasing temperature in both hemispheres (Figure 1E and Figure S2). Neuronal activity was less affected as distance increased between the recording sites and the cooling plate (Figure S2), so that the cooling effect was restricted to SEF. In total, we performed 31 bilateral inactivation sessions (Monkey A: 16 sessions and Monkey I: 15 sessions), with an average of 1399 successful trials and 7 periods of inactivation per session.

The effect of SEF inactivation on risky choice was highly consistent across the two monkeys. During inactivation, we observed in both monkeys some small changes in saccade metrics (Figure S3), fixation stability (Figure S3) and reaction times (S4A and Table S3), consistent with previous findings [27–30]. These changes in oculomotor behavior were too small to affect choice. SEF inactivation caused only small and inconsistent changes in error rate when the options only differed in either winning probability or magnitude (Figure 3A). Therefore, SEF inactivation did not affect the ability of the monkeys to use the visual cues for economically rational choices. Nevertheless, both monkeys showed a significantly altered pattern of choice during SEF inactivation: they were consistently less risk seeking (Figure 3 C and E). The monkeys showed reduced risk preference in 90% (28/31) of inactivation sessions as measured by the risk-value and prospect theory models.

In the risk-value model, the risk term (Var) coefficients were significantly smaller during inactivation compared to the control condition (Figure 3C, paired t-test, Combined: $\overline{\Delta\beta_{var}}$ = 1.21, p= 9.92×10^{-6}; Monkey A: $\overline{\Delta\beta_{var}}$ = 0.86, p= 0.02; Monkey I: $\overline{\Delta\beta_{var}}$ = 1.59, p= 1.23×10^{-4}). Thus, both monkeys showed a strong reduction of risk preference during inactivation (Combined: $\overline{\Delta\beta_{var}}/\overline{\beta_{var}}$ = 35%; Monkey A: $\overline{\Delta\beta_{var}}/\overline{\beta_{var}}$ = 20%; Monkey I: $\overline{\Delta\beta_{var}}/\overline{\beta_{var}}$ = 60%). For gambles with identical EV, both monkeys chose the higher risk option significantly less often (Figure 3B, paired t-test, Combined: ΔP(choose higher risk option)=

Author Manuscript

Author Manuscript

Author Manuscript

Author Manuscript

6.97%, p= 1.46×10^{-3}; Monkey A: ΔP(choose higher risk option)= 4.29%, p= 0.05; Monkey I: ΔP(choose higher risk option)= 9.66%, p= 0.01). The monkeys' choices were also less determined by EV differences during inactivation (Figure 3D, paired t-test, Combined: $\overline{\Delta\beta_{EV}}$ = 0.90, $\overline{\Delta\beta_{EV}}/\overline{\beta_{EV}}$ = 16%, p= 0.01; Monkey A: $\overline{\Delta\beta_{EV}}$ = 1.10, $\overline{\Delta\beta_{EV}}/\overline{\beta_{EV}}$ = 21%, p= 0.01; Monkey I: $\overline{\Delta\beta_{EV}}$ = 0.70, $\overline{\Delta\beta_{EV}}/\overline{\beta_{EV}}$ = 11%, p= 0.18). Across all trials, the monkeys chose the smaller EV option significantly more often (paired t-test, Combined: P(choose lower EV option)= 1.71%, p= 3.63×10^{-4}; Monkey A: P(choose lower EV option)= 1.46%, p= 5.39×10–3; Monkey I: ΔP(choose lower EV option)= 1.97%, p= 0.02). However, this effect was less pronounced than the one resulting from the lower preference for risk (Figure S4B).

In the prospect theory model, the utility functions of both monkeys were less convex during inactivation (Figure 3 E and G, paired t-test, Combined: $\overline{\Delta\rho}$ = −0.11, p=6.32×10^{-6}; Monkey A: $\overline{\Delta\rho}$ = −0.08, p= 2.00×10^{-3}; Monkey I: $\overline{\Delta\rho}$ = −0.14, p=7.35×10^{-4}). The monkeys showed less overestimation of high reward amounts during inactivation. In contrast, the probability weighting function, which captures the monkeys' estimation of the probability of winning, remained unchanged (Figure 3 F and G, paired t-test, Combined: $\overline{\Delta\alpha}$ = −0.09, p= 0.17; Monkey A: $\overline{\Delta\alpha}a$ = 0.02, p= 0.59; Monkey I: $\overline{\Delta\alpha}$ = −0.08, p= 0.06).

We tested if changes in motor strategies could explain this preference change, since manipulation of dopaminergic receptors in frontal eye field can change positional bias and the tendency to repeat actions [31]. There was no significant change of directional preference (risk-value model: t-test, Combined: p=0.19; Monkey A: p=0.06; Monkey I: p=0.01; prospect theory model: t-test, Combined: p=0.31; Monkey A: p=0.06; Monkey I: p=0.23) or repetition of the previous choice direction (Combined: p=0.21; Monkey A: p=0.91; Monkey I: p=0.16). The reduced risk-seeking reflects therefore a true change in choice preference.

SEF inactivation increases trial desertion after gamble loss

During the result epoch, SEF neurons encode reward prediction error (RPE), the difference between expected and actual reward [6]. RPE signals are thought to guide reinforcement learning and updating of action value signals [6,31]. We therefore tested whether SEF inactivation influenced the monkeys' sensitivity to these locally encoded RPE signals. Following the loss of a gamble, both monkeys occasionally actively broke fixation by making a saccade outside of the fixation window (Figure S3C), thus deserting the trial before reward delivery. This behavior was maladaptive, because it did not change the outcome of the trial, and substantially prolonged the time until reward delivery, as well as the time until the next chance to make a choice. Trial desertion developed spontaneously, was sensitive to negative RPE, and increased with larger errors (Figure 4A). Interestingly, desertion rate was significantly higher in choice trials than no-choice trials (paired t-test, Combined: $\overline{\Delta\alpha}$ = 0.03, p= 4.73×10^{-4}; Monkey A: $\overline{\Delta\alpha}$ =0.02, p= 0.02; Monkey I: $\overline{\Delta\alpha}$ = 0.04, p= 0.01). Following SEF inactivation, both monkeys were substantially more sensitive to RPE in choice trials (Figure 4 A and B top, paired t-test, Combined: $\overline{\Delta\alpha}$ = −0.11, p= 9.35×10^{-9}; Monkey A: $\overline{\Delta\alpha}$ = −0.06 p=1.82×10^{-4}; Monkey I: $\overline{\Delta\alpha}$ = −0.16 p= 1.85×10^{-7}), but not in no-choice trials (Figure 4 A and B bottom, paired t-test, Combined: $\overline{\Delta\alpha}$ = −0.02, p=

Author Manuscript Author Manuscript Author Manuscript Author Manuscript

0.06; Monkey A: $\overline{\Delta\alpha}$ =−0.02, p= 0.16; Monkey I: $\overline{\Delta\alpha}$ = −0.02, p= 0.21.) In addition, desertion rates alsosignificantly increased in all other task epochs of choice trials during inactivation (Figure S4). Thus, outcome monitoring signals in the SEF were not necessary to drive desertion behavior. On the contrary, SEF activity seems to be necessary to suppress desertion behavior throughout the task, but in particular following aversive events following free choices (Figure 4 A and B).

SEF inactivation does not affect reward-history dependent adjustments of risk preference

Both monkeys showed a significant change of risk preference depending on the preceding gamble outcome. They were less risk seeking when they had lost the previous gamble than when they had won it. In the risk-value model, this manifested itself in a significant difference in the Var coefficient (Figure 4C,paired t-test, Combined: $\overline{\Delta\beta_{var}}$ = 0.38, p= 0.03; Monkey A: $\overline{\Delta\beta_{\mathrm{var}}}$ = 0.25, p= 0.10; Monkey I: $\overline{\Delta\beta_{CV}}$ = 0.50, p= 0.09), while the EV coefficient was not significantly different (paired t-test, Combined: $\overline{\Delta\beta_{EV}}$ = −0.46, p= 0.11; Monkey A: $\overline{\Delta\beta_{EV}}$ = 0.16, p= 0.45; Monkey I: $\overline{\Delta\beta_{EV}}$ = −1.09, p= 0.14). In the prospect theory model, the same change in risk preference manifested itself in less convex utility functions (paired t-test, Combined: $\overline{\Delta\rho}$ = 0.03, p= 0.05; Monkey A: $\overline{\Delta\rho}$ = 0.03, p= 0.06; Monkey I: $\overline{\Delta\rho}$ = 0.04, p= 0.27) and in a more linear probability weighting function (paired t-test, Combined: $\overline{\Delta\alpha}$ = −0.06, p= 0.01; Monkey A: $\overline{\Delta\alpha}$ = −0.04, p= 0.09; Monkey I: $\overline{\Delta\alpha}$ = −0.08, p= 0.01) after losing in the previous trial. Thus, following a loss, both monkeys were more risk averse in their subsequent choice. However, this gamble outcome effect persisted during SEF inactivation and did not show any significant changes (Figure 4D, paired t-test, $\overline{\Delta(\Delta\beta_{EV})}$ = 0.09, p= 0.77; $\overline{\Delta(\Delta\rho)}$= −0.02, p= 0.62; $\overline{\Delta(\Delta\alpha)}$= 0.01, p= 0.82). Therefore, although gamble outcome history modulates the monkeys' gamble value estimation, this adjustment does not depend on local RPE signals in SEF.

Discussion

Decision related activity has been observed in many brain regions [32]. However, it remains unknown whether this activity is causally related to the decision process [33–35]. Here we showed that the SEF, an oculomotor area within the medial frontal cortex, does play a causal role in regulating risky and impulsive behavior in oculomotor decisions.

SEF is only one among a number of cortical [1,13,15,36] and subcortical [14,37–39] brain areas that contribute to decision-making under risk. However, the effect of SEF inactivation is not a simple decrease in decision accuracy, as would be expected if SEF operates in parallel with other areas that contain redundant signals, so that SEF inactivation merely reduces the overall strength of the decision variable. Instead, SEF seems to selectively mediate the effect of risk preferences, but not expected value, on choice. Eliminating these signals cannot be fully compensated for by other parts of the decision-making circuit.

Risk preference is often seen as a fundamental, stable personality trait [40]. However, the risk preference of individuals can vary substantially across different behavioral domains [41]. Even when tested only within the financial domain, risk preference varies [42]. These

Author Manuscript Author Manuscript Author Manuscript Author Manuscript

findings suggest that risk preference is not a stable personality trait, but rather emerges during decision-making in a context-dependent manner. Risk-attitude depends on beliefs about the environment, the set of available options, and the contingencies governing action outcomes [43]. In the context of our experimental task, the small stakes and large number of trials likely reduced the averseness of losing a gamble and thus induced risk-seeking behavior [42,43]. These contextual factors are not directly observable and must be inferred. Nevertheless, they are important elements of a cognitive representation of task space [46]. A recent study [43] shows that rhesus monkeys show very different utility and probability weighting functions when tested with different gamble tasks. This supports the hypothesis of the use of flexible cognitive processes in constructing risk attitudes in a context-dependent fashion.

A number of cortical areas might be important in influencing risk-attitude. Orbital frontal cortex (OFC) is involved in representing task space [47,48] and contains risk selective neurons [10,36]. Recent lesion experiments in macaques indicate also a role of ventrolateral prefrontal cortex (VLPFC) in learning and encoding the probability of reward outcomes [49]. In addition, ACC has also been shown to be correlated with risk uncertainty [12–14]. SEF receives synaptic input from frontal areas including OFC, VLPFC, and ACC, and projects to the frontal eye field, and superior colliculus [50]. It integrates sensory and task context information to guide the selection of appropriate actions [5]. Thus, the effect of SEF inactivation likely reflects the diminished influence of these belief states about the task structure, so that the subjective value of a gamble option is less determined by risk preference.

Perturbations of dopaminergic activity can also modulate risky choices [37,51–53]. In rodents, ventral tegmental area stimulation after non-rewarded choices increased subsequent willingness to choose a risky gamble [51]. In contrast to modulating risk preference by changing cognitive processes, these perturbations likely change choice behavior by modulating EV updates using model-free learning mechanisms. The fact that SEF inactivation does not affect reward-history dependent EV adjustments suggests the independent contributions of two different brain circuits to the evaluation of uncertain reward options: risk preference is associated with a goal-directed frontal cortex-based circuit, including SEF, while EV representation is associated with a more automatic subcortical circuit.

The monkeys sometimes desert the trial following an unexpected loss. This behavior likely represents an automatic response to the aversive outcome, especially following free choices. The fact that SEF inactivation increased this behavior, but only during free choice trials, cannot be explained by the fixation quality during inactivation (Figure S3 and Methods). Instead, it suggests that SEF activity contributes to self-control by suppressing automatic, but maladaptive, responses and promoting behavior that maximizes long-term reward. Such a role would be consistent with the well-known contribution of SEF to other forms of executive control [5,54].

In conclusion, our results demonstrate for the first time the causal role of SEF in mediating the effect of risk preference on decisions under uncertainty. These findings provide new

Author Manuscript

Author Manuscript

Author Manuscript

Author Manuscript

insight into the neuronal circuits underlying inconsistent, context dependent choices under risk observed across humans [18,42,55] and non-human primates [45], and may provide the basis for more effective treatments of highly maladaptive impulsive risky behaviors.

STAR Methods:

KEY RESOURCES TABLE

REAGENT or RESOURCE	SOURCE	IDENTIFIER
Experimental Models: Organisms/Strains		
Macaca mulatta	Johns Hopkins University	N/A
Software and Algorithms		
MATLAB Statistics and Machine Learning Toolbox, R2016b, R2017b	Mathworks	https://www.mathworks.com/products/matlab.html
Online Sorter, Version 3.0	Plexon	https://plexon.com/products/offline-sorter/
Other		
SR Research Eyelink Eye Tracker, Eyelink 1000 Plus	Eyelink	http://www.sr-research.com

CONTACT FOR REAGENT AND RESOURCE SHARING

Further information and requests for resources should be directed to and will be fulfilled by the Lead Contact, Veit Stuphorn (veit@jhu.edu).

EXPERIMENTAL MODEL AND SUBJECT DETAILS

All animal care and experimental procedures were in compliance with the US Public Health Service policy on the humane care and use of laboratory animals, and were approved by Johns Hopkins University Animal Care and Use Committee. Two male rhesus monkeys (Macaca mulatta, Monkey A: 7.5 kg, Monkey I: 7.2 kg) were trained to perform the tasks used in this study. After training, we placed a hexagonal chamber (29 mm in diameter) centered over the midline, 28 mm (Monkey A) and 27 mm (Monkey I) anterior of the interaural line.

METHOD DETAILS

Electrophysiological techniques.

During each bilateral inactivation session, single units were recorded using two tungsten microelectrodes with an impedance of 2–4 MΩs (Frederick Haer, Bowdoinham, ME), one in each hemisphere (Figure 1C). The microelectrodes were advanced, using a self-built microdrive system. Data were collected using the PLEXON system (Plexon, Inc., Dallas, TX). The electrodes penetrated the cortex perpendicular to the surface of the SEF. The depths of the neurons were estimated by their recording locations relative to the surface of the cortex.

Author Manuscript

Author Manuscript

Author Manuscript

Author Manuscript

Behavioral task.

In the task, the monkeys had to make saccades to peripheral targets that were associated with different reward amounts and probabilities (Figure 1A). The targets were colored squares, 2.25×2.25° in size. They were always presented 10° away from the central fixation point at a 45, 135, 225, or 315° angle. There were 7 different gamble targets (Figure 1B), each consisting of two colors corresponding to the two possible reward amounts. The portion the target filled with each color corresponded to the probability of receiving the corresponding reward amount. Four different colors indicated four different reward amounts (increasing from 1, 3, 5 to 9 units of water, where 1 unit equaled 30 μl). The minimum reward amount for the gamble option was always 1 unit of water (indicated by cyan), while the maximum reward amount ranged from 3 (red), 5 (blue) to 9 units (green), with three different probabilities of receiving the maximum reward outcome (20, 40, and 80%). Only gamble options from either option matrix1 or option matrix 2 were used in an experimental session.

The task consisted of two types of trials - choice and no-choice trials. All trials started with the appearance of a fixation point at the center of the screen (Figure 1C), on which the monkeys were required to fixate for 500–1000 ms. In choice trials, two targets appeared in two locations that were randomly chosen from across the four quadrants (resulting in 12 distinct possible spatial configurations for each pair of gamble options). Simultaneously, the fixation point disappeared, which indicated to the monkeys that they were now free to choose between the gambles by making a saccade toward one of the targets. Following the choice, the non-chosen target disappeared from the screen. The monkeys were required to keep fixating on the chosen target for 500–600ms, after which the gamble outcome was revealed. The two-colored square changed into a single-colored square associated with the final reward amount. The monkeys were required to continue to fixate on the target for another 300 to 600 ms, during which the result cue was still displayed, until the reward was delivered. We observed quantitatively similar results using both option matrices (Figure S1). We therefore report the combined results in the manuscript. All 7 gamble options in each option matrix were systematically paired with all other options from that matrix. This resulted in 21 different combinations of gamble options in choice trials. The sequence of events in no-choice trials was the same as in choice trials, except that only one target was presented. In these trials, the monkeys had to make a saccade to the given target in order to get the fluid reward.

If the monkey deserted a choice trial before choosing between the gambles, the choice trial was simply repeated. However, if the monkey deserted the trial after the choice, but before reward was delivered, the next trial was an unscheduled no-choice trial. The target shown on this no-choice trial depended on the stage at which the monkey had deserted the preceding trial. If the monkey had deserted before the gamble result was revealed, the target was the previously chosen gamble option. If the monkey had deserted the trial after the gamble result was shown, the target was the previously indicated sure reward that was the gamble outcome. Thus, a gamble option or result was binding, once it was chosen or revealed, respectively. Accordingly, desertion behavior was suboptimal and only reduced the average reward rate across trials.

Author Manuscript

Author Manuscript

Author Manuscript

Author Manuscript

Cryogenic inactivation apparatus and procedure.

To determine the location of the SEF, we obtained magnetic resonance images (MRI) for Monkey A and Monkey I. We used the location of the branch of the arcuate sulcus as an anatomical landmark. Before the inactivation experiment, we identified the SEF by neurophysiology recordings (Figure 1C). In both monkeys, we found neurons active during the saccade preparation period in the region from 0 to 11 mm anterior to the genu of the arcuate branch and within 5 mm to 2 mm of the longitudinal fissure. We designated the cortical areas with saccade-preparation related activity as belonging to the SEF [8], consistent with previous studies from our lab and existing literature [44,56].

Cooling plates (Figure 1C) were used to inactivate the SEF bilaterally (10mm from anterior to posterior and 12mm from left to right). This method allows us to rapidly and repeatedly inactivate a large and confined surface cortical area [24,57]. The cooling method followed the design by Lomber et al. [24]. Room temperature methanol was pumped through Teflon tubing that passed through a dry ice bath, in which it was reduced to subzero temperature. The chilled methanol was then pumped through a cryoloop attached to a stainless-steel plate placed over the dura, which cooled down the underlying cortical tissue. The methanol was then returned to the same reservoir from which it came to form a closed loop. The cortical temperature on the dura was monitored by a micro-thermocouple attached to the cooling plate. At the same time, two electrodes recorded cortical activity in the left and right hemisphere. During each session, monkeys initially performed the task for 10–15 min in the control state. Then the SEF region was deactivated bilaterally for 10–15 min by pumping chilled methanol through the cryoloop while the task continued. The cortical temperature returned quickly to normal after switching off the methanol pump (Figure 1E), while the monkey continuously performed the task. This whole process was repeated throughout the experimental session and resulted on average in 1399 successful trials, which is on average 7 repetitions of control/inactivation cycles. In the control state, the temperature measured at the cooling probe was 35–39 ºC. During the inactivation state, the temperature at the cooling plate was reduced to 0–15 ºC. Transition trials, right after turning on the pump and turning off the pump, with the temperature between 34 and 16 °C, were not used in the behavioral analysis. The monkeys were sitting in an acoustic noise-isolated chamber. The methanol pump was placed outside this chamber.

QUANTIFICATION AND STATISTICAL ANALYSIS

In general, two-tailed t-tests were used for statistical tests, unless specified otherwise.

Risk behavior analysis.

Trial-by-trial data was collected during control and inactivation. We quantified the monkeys' risk behavior using two types of risk models: risk-value models and prospective theory models. All reported p values regarding mean differences between control and inactivation conditions are results of two-tailed paired t-tests. P values relating to gamble history effects are based on one-tailed paired t-tests.

Author Manuscript

Author Manuscript

Author Manuscript

Author Manuscript

The **risk-value model** is derived from financial theory [16] and represents the value of a gamble as the sum of multiple terms related to the distribution of possible gamble outcomes. The first term is the mean value of the gamble outcome distribution (i.e., the expected value of the gamble). The second term is the variance of the gamble outcomes (i.e., variance risk). The sign of this term determines if outcome variance increases (risk-seeking) or decreases (risk-averse) the value of gambles. In the following, we will refer to this second component simply as risk. In more complex models of this type, higher statistical moments describing the outcome distribution (skewness, kurtosis) are also taken into account. However, here we will not use these higher-order terms.

We used logistic regression to quantify the ability of the risk-value model to predict choice behavior. We assumed that choice depended in a stochastic fashion on the difference in subjective value between the two gamble options. We used a soft-max decision function to model this aspect of behavior:

$$h_\beta(x) = \frac{1}{1 + e^{(-\beta^T x)}} \quad (1)$$

such that:

$$h_\beta(x) = P(y = 1 \mid x; \beta) \quad (2)$$

where $y \in \{0,1\}$ is a dummy variable indicating whether the monkeys choose the first option or not, and β is the set of weights learned by the model. The first option is defined as the left option if the choice options were on both left and right visual field, and is defined as the up option if the choice options were both on the same visual field. The full risk-value model has two terms: expected value (EV) and outcome variance (Risk, Var). Expected value is defined as the arithmetic mean of the outcomes: $\mathrm{EV} = \mathrm{V}_{win} \times p_{win} + \mathrm{V}_{loss} \times p_{loss}$, with V_{win} denoting the winning reward magnitude, V_{loss} denoting the losing reward magnitude, p_{win} denoting the winning probability, and p_{loss} denoting the losing probability. We defined risk as the variance of the gamble option [17]: $\mathrm{Var} = ((V_{win} - V_{loss}) \times \sqrt{p_{win}(1 - p_{win})})$ and coefficient of variance [21]: $\mathrm{CV} = ((V_{win} - V_{loss}) \times \sqrt{p_{win}(1 - p_{win})})/EV$ (Table S1). We achieved slightly better behavioral fitting by using standard deviation than coefficient of variance (Table S2). We tested three variants of the risk-value model, whereby subjective value of a gamble depended only on: (3) expected value, (4) risk, (5) or both (the full model):

$$\beta^T x = \beta_D + \beta_{EV}(\mathrm{EV}_1 - \mathrm{EV}_2) \quad (3)$$

Author Manuscript

Author Manuscript

Author Manuscript

Author Manuscript

$$\beta^T x = \beta_D + \beta_{Var}(Var_1 - Var_2) \quad (4)$$

$$\beta^T x = \beta_D + \beta_{Var}(Var_1 - Var_2) + \beta_{EV}(\mathrm{EV}_1 - \mathrm{EV}_2) \quad (5)$$

Comparing the predictions of the three versions with trial-by-trial choices of the monkey allowed us to determine, if both factors were necessary to predict choice behavior. In order to quantify the tendency of choosing the same direction as in the previous trial, we added an additional parameter which represent whether the choice option appear at the previous chosen direction or not for both choice options.

$$\beta^T x = B_D + \beta_{Var}(Var_1 - Var_2) + \beta_{EV}(EV_1 - EV_2) + \beta_r(R_1 - R_2) \quad (6)$$

R_i is 1 if the location of the option i is the same as the chosen direction in the previous trial, and R_i is 0 if the location of the option i is different.

We used the gradient descent algorithm to minimize the cost function, which represents negative log-likelihood function, over training examples:

$$J(\beta) = -\frac{1}{m}\left(\sum_{i=1}^{m} y_i \log(h_\beta(x_i)) + (1 - y_i)\log(1 - h_\beta(x_i))\right) \quad (7)$$

Both EV and Var were normalized to [0, 1] to enable the comparison among different independent variables. β_D represents the directional bias. The regression coefficient for Var indicates the risk attitude. A negative sign of the coefficient indicated that increased outcome variance reduced subjective value, indicating risk-aversion, while a positive sign indicated risk-seeking.

Prospect theory is derived from classical expected value theory in economics [18] and assumes that the subjective value of a gamble depends on the utility of the reward amount that can be earned, weighted by the ‘subjective’ estimation of the probability of the particular outcome. Both the utility function and the probability function can be non-linear and thus might influence risk preference. Prospect theory also makes the assumption that utilities are perceived in a relative framework (i.e., as gains or losses relative to a reference point), not an absolute framework (i.e., the total amount of earned reward). However, this aspect of the model is irrelevant for our study, because the monkey does not encounter negative outcomes, so that for each individual trial the relative and absolute reference frame make identical predictions.

We assumed again a soft-max decision function where the probability of selecting the gamble was indicated by the difference of the subjective value of the two options:

Author Manuscript Author Manuscript Author Manuscript Author Manuscript

$$h(\Delta U) = \frac{1}{1 + e^{(-(\Delta U) + d)}} \quad (8)$$

where $\Delta U = U_1 - U_2$ is the utilities difference between gamble options, and d is the directional bias between two options. The utility of the choice option i was calculated as following:

$$U_i = u_\rho\left(V_{win_i}\right) \times w_\alpha\left(p_{win_i}\right) + u_\rho\left(V_{loss_i}\right) \times w_\alpha\left(p_{loss_i}\right) \quad (9)$$

where $u_\rho(V)$ is a power function to model the utility function, following previous research [9,22]:

$$u_\rho(V) = V^\rho \quad (10)$$

and $w_\alpha(p)$ is a 1-parameter Prelec function to model the probability weighting function, as commonly done [9,22,23,58]:

$$w_\rho(p) = e^{(-(-\ln(p))^\alpha)} \quad (11)$$

ρ in equation (10), α in equation (10) and d in equation (8) were free parameters optimized by a Nelder-Mead search algorithm to minimize the sum of negative log likelihoods with respect to the utility function. As in classical expected value theory in economics [22], a convex utility function ($\rho > 1$) implies risk seeking, because in this scenario, the subject values large reward amounts disproportionally more than small reward amounts. Gain from winning the gamble thus has a stronger influence on choice than loss from losing the gamble. In the same way, a concave utility function ($\rho < 1$) implies risk seeking, because large reward amounts are valued disproportionally less than small ones. Independently, a non-linear weighting of probabilities can also influence risk attitude. For example, a S-shaped probability weighting function ($\alpha < 1$) implies that the subject overweighs small probabilities and underweights the large probabilities. This would lead to higher willingness to accept a risky gamble, because small probabilities to win large amounts would be overweighted relative to high probabilities to win moderate amounts.

As with the variability risk model, we tested three variants of the prospect theory model: 1) a full model, in which both utility function and weighting function were allowed to be non-linear, 2) a ‘utility-only’ version, in which only the utility function was allowed to be non-linear, and 3) a ‘probability weighting only’ version, in which only the probability weighting function was allowed to be non-linear.

Author Manuscript

Author Manuscript

Author Manuscript

Author Manuscript

Model comparison.

The Bayesian information criterion [59,60] was used for model comparison.

$$BIC = k \times log(n) - 2log(L) \quad (12)$$

where log(L) is the log-likelihood (LL) of the model, n is the number of trials. k is the number of free parameters to be estimated.

In addition, we also combined all the trials across different experiment sessions from one monkey in a given task together. We then performed five-fold cross-validation method with different models based [43]. During cross-validation, we randomly divided all the trials into training set (80%) and test set (20%). We used training set to optimize the parameters for a given model, and use the test set to calculate LL to evaluate the model (Table S3). Cross validation procedures were repeated 50 times independently for each monkey per task.

Desertion Behavior.

We used an exponential function to quantify the monkeys' desertion behavior as a function of reward prediction error during the result period:

$$p(desertion) = a * e^{(-a * x)} \quad (13)$$

where a is the rate parameter. Paired t-tests were used to test for significance of any difference in desertion rate in the control and inactivation condition.

Supplementary Material

Refer to Web version on PubMed Central for supplementary material.

Acknowledgements

The authors would like to thank Xiaoqin Wang, Marcus Jeschke, Bill Nash and Bill Quinlan for technical help, Tirin Moore and William Newsome for invaluable scientific discussion, and Christof Fetsch, Marc Zirnsak, Donatas Jonikaitis, and Megan Wang for comments on the manuscript. This work was supported by the National Institutes of Health through grants 2R01NS086104 and 1R01DA040990 to VS.

References

1. Schultz W (2017). Neuronal Risk Processing in Human and Monkey Prefrontal Cortex. In The Prefrontal Cortex as an Executive, Emotional, and Social Brain (Springer), pp. 103–131.
2. Roesch MR, and Olson CR (2003). Impact of expected reward on neuronal activity in prefrontal cortex, frontal and supplementary eye fields and premotor cortex. J. Neurophysiol 90, 1766–1789. [PubMed: 12801905]
3. Lee D, Seo H, and Jung MW (2012). Neural basis of reinforcement learning and decision making. Annu. Rev. Neurosci 35, 287–308. [PubMed: 22462543]
4. Middlebrooks PG, and Sommer MA (2012). Neuronal correlates of metacognition in primate frontal cortex. Neuron 75, 517–530. [PubMed: 22884334]
5. Stuphorn V (2015). The role of supplementary eye field in goal-directed behavior. J. Physiol.-Paris 109, 118–128. [PubMed: 25720602]

Author Manuscript

Author Manuscript

Author Manuscript

Author Manuscript

6. So N, and Stuphorn V (2012). Supplementary eye field encodes reward prediction error. J. Neurosci 32, 2950–2963. [PubMed: 22378869]
7. So N, and Stuphorn V (2015). Supplementary eye field encodes confidence in decisions under risk. Cereb. Cortex 26, 764–782. [PubMed: 25750256]
8. Chen X, and Stuphorn V (2015). Sequential selection of economic good and action in medial frontal cortex of macaques during value-based decisions. Elife 4, e09418. [PubMed: 26613409]
9. Hsu M, Krajbich I, Zhao C, and Camerer CF (2009). Neural response to reward anticipation under risk is nonlinear in probabilities. J. Neurosci 29, 2231–2237. [PubMed: 19228976]
10. O'Neill M, and Schultz W (2010). Coding of reward risk by orbitofrontal neurons is mostly distinct from coding of reward value. Neuron 68, 789–800. [PubMed: 21092866]
11. Raghuraman AP, and Padoa-Schioppa C (2014). Integration of multiple determinants in the neuronal computation of economic values. J. Neurosci 34, 11583–11603. [PubMed: 25164656]
12. Amiez C, Joseph JP, and Procyk E (2006). Reward encoding in the monkey anterior cingulate cortex. Cereb Cortex 16, 1040–55. [PubMed: 16207931]
13. Christopoulos GI, Tobler PN, Bossaerts P, Dolan RJ, and Schultz W (2009). Neural correlates of value, risk, and risk aversion contributing to decision making under risk. J. Neurosci 29, 12574–12583. [PubMed: 19812332]
14. Monosov IE (2017). Anterior cingulate is a source of valence-specific information about value and uncertainty. Nat. Commun 8, 134. [PubMed: 28747623]
15. Tobler PN, Christopoulos GI, O'Doherty JP, Dolan RJ, and Schultz W (2009). Risk-dependent reward value signal in human prefrontal cortex. Proc. Natl. Acad. Sci 106, 7185–7190. [PubMed: 19369207]
16. Markowitz H (1952). The utility of wealth. J. Polit. Econ 60, 151–158.
17. Stiglitz JE, and Rothschild M (1970). Increasing risk: I. A definition. J. Econ. Theory 2, 225–243.
18. Kahneman D, and Tversky A (2013). Prospect theory: An analysis of decision under risk. In HANDBOOK OF THE FUNDAMENTALS OF FINANCIAL DECISION MAKING: Part I (World Scientific), pp. 99–127.
19. McCoy AN, and Platt ML (2005). Risk-sensitive neurons in macaque posterior cingulate cortex. Nat. Neurosci 8, 1220–1227. [PubMed: 16116449]
20. Kim S, Bobeica I, Gamo NJ, Arnsten AF, and Lee D (2012). Effects of α−2A adrenergic receptor agonist on time and risk preference in primates. Psychopharmacology (Berl.) 219, 363–375. [PubMed: 21979441]
21. Weber EU, Shafir S, and Blais A-R (2004). Predicting risk sensitivity in humans and lower animals: risk as variance or coefficient of variation. Psychol. Rev 111, 430. [PubMed: 15065916]
22. Lattimore PK, Baker JR, and Witte AD (1992). The influence of probability on risky choice: A parametric examination. J. Econ. Behav. Organ 17, 377–400.
23. Stauffer WR, Lak A, Bossaerts P, and Schultz W (2015). Economic choices reveal probability distortion in macaque monkeys. J. Neurosci 35, 3146–3154. [PubMed: 25698750]
24. Lomber SG, Payne BR, and Horel JA (1999). The cryoloop: an adaptable reversible cooling deactivation method for behavioral or electrophysiological assessment of neural function. J. Neurosci. Methods 86, 179–194. [PubMed: 10065985]
25. Benita M, and Condé H (1972). Effects of local cooling upon conduction and synaptic transmission. Brain Res 36, 133–151. [PubMed: 4332736]
26. Lomber SG, Cornwell P, Sun J-S, MacNeil MA, and Payne BR (1994). Reversible inactivation of visual processing operations in middle suprasylvian cortex of the behaving cat. Proc. Natl. Acad. Sci 91, 2999–3003. [PubMed: 8159694]
27. Sommer MA, and Tehovnik EJ (1999). Reversible inactivation of macaque dorsomedial frontal cortex: effects on saccades and fixations. Exp. Brain Res 124, 429–446. [PubMed: 10090655]
28. Schiller PH, and Chou I -ha. (2000). The effects of anterior arcuate and dorsomedial frontal cortex lesions on visually guided eye movements: 2. Paired and multiple targets. Vision Res 40, 1627–1638. [PubMed: 10788662]
29. Parton A, Malhotra P, and Husain M (2004). Hemispatial neglect. J. Neurol. Neurosurg. Psychiatry 75, 13–21. [PubMed: 14707298]

Author Manuscript

Author Manuscript

Author Manuscript

Author Manuscript

30. Parton A, Nachev P, Hodgson TL, Mort D, Thomas D, Ordidge R, Morgan PS, Jackson S, Rees G, and Husain M (2007). Role of the human supplementary eye field in the control of saccadic eye movements. Neuropsychologia 45, 997–1008. [PubMed: 17069864]
31. Stuphorn V, Taylor TL, and Schall JD (2000). Performance monitoring by the supplementary eye field. Nature 408, 857–860. [PubMed: 11130724]
32. Schultz W (2015). Neuronal Reward and Decision Signals: From Theories to Data. Physiol. Rev 95, 853–951. [PubMed: 26109341]
33. Guo ZV, Li N, Huber D, Ophir E, Gutnisky D, Ting JT, Feng G, and Svoboda K (2014). Flow of cortical activity underlying a tactile decision in mice. Neuron 81, 179–194. [PubMed: 24361077]
34. Erlich JC, Brunton BW, Duan CA, Hanks TD, and Brody CD (2015). Distinct effects of prefrontal and parietal cortex inactivations on an accumulation of evidence task in the rat. Elife 4, e05457.
35. Hanks TD, Kopec CD, Brunton BW, Duan CA, Erlich JC, and Brody CD (2015). Distinct relationships of parietal and prefrontal cortices to evidence accumulation. Nature 520, 220–223. [PubMed: 25600270]
36. O'Neill M, and Schultz W (2013). Risk prediction error coding in orbitofrontal neurons. J. Neurosci 33, 15810–15814. [PubMed: 24089488]
37. Zalocusky KA, Ramakrishnan C, Lerner TN, Davidson TJ, Knutson B, and Deisseroth K (2016). Nucleus accumbens D2R cells signal prior outcomes and control risky decision-making. Nature 531, 642–646. [PubMed: 27007845]
38. Leong JK, Pestilli F, Wu CC, Samanez-Larkin GR, and Knutson B (2016). White-matter tract connecting anterior insula to nucleus accumbens correlates with reduced preference for positively skewed gambles. Neuron 89, 63–69. [PubMed: 26748088]
39. Ledbetter NM, Chen CD, and Monosov IE (2016). Multiple mechanisms for processing reward uncertainty in the primate basal forebrain. J. Neurosci 36, 7852– 7864. [PubMed: 27466331]
40. Gilaie-Dotan S, Tymula A, Cooper N, Kable JW, Glimcher PW, and Levy I (2014). Neuroanatomy predicts individual risk attitudes. J. Neurosci 34, 12394– 12401. [PubMed: 25209279]
41. Weber EU, Blais A-R, and Betz NE (2002). A domain-specific risk-attitude scale: Measuring risk perceptions and risk behaviors. J. Behav. Decis. Mak 15, 263– 290.
42. Pedroni A, Frey R, Bruhin A, Dutilh G, Hertwig R, and Rieskamp J (2017). The risk elicitation puzzle. Nat. Hum. Behav 1, 803.
43. Farashahi S, Azab H, Hayden B, and Soltani A (2018). On the flexibility of basic risk attitudes in monkeys. J. Neurosci, 2260–17.
44. So N-Y, and Stuphorn V (2010). Supplementary eye field encodes option and action value for saccades with variable reward. J. Neurophysiol 104, 2634–2653. [PubMed: 20739596]
45. Heilbronner SR, and Hayden BY (2013). Contextual factors explain risk-seeking preferences in rhesus monkeys. Front. Neurosci 7.
46. Daw ND, Gershman SJ, Seymour B, Dayan P, and Dolan RJ (2011). Model-based influences on humans' choices and striatal prediction errors. Neuron 69, 1204– 15. [PubMed: 21435563]
47. Chan SC, Niv Y, and Norman KA (2016). A probability distribution over latent causes, in the orbitofrontal cortex. J. Neurosci 36, 7817–7828. [PubMed: 27466328]
48. Schuck NW, Cai MB, Wilson RC, and Niv Y (2016). Human orbitofrontal cortex represents a cognitive map of state space. Neuron 91, 1402–1412. [PubMed: 27657452]
49. Rudebeck PH, Saunders RC, Lundgren DA, and Murray EA (2017). Specialized representations of value in the orbital and ventrolateral prefrontal cortex: desirability versus availability of outcomes. Neuron 95, 1208–1220. [PubMed: 28858621]
50. Huerta MF, and Kaas JH (1990). Supplementary eye field as defined by intracortical microstimulation: connections in macaques. J. Comp. Neurol 293, 299– 330. [PubMed: 19189718]
51. Stopper CM, Maric TL, Montes DR, Wiedman CR, and Floresco SB (2014). Overriding phasic dopamine signals redirects action selection during risk/reward decision making. Neuron 84, 177–189. [PubMed: 25220811]
52. Nasrallah NA, Clark JJ, Collins AL, Akers CA, Phillips PE, and Bernstein IL (2011). Risk preference following adolescent alcohol use is associated with corrupted encoding of costs but not rewards by mesolimbic dopamine. Proc. Natl. Acad. Sci 108, 5466–5471. [PubMed: 21402915]

Author Manuscript

Author Manuscript

Author Manuscript

Author Manuscript

53. Onge JRS, Abhari H, and Floresco SB (2011). Dissociable contributions by prefrontal D1 and D2 receptors to risk-based decision making. J. Neurosci 31, 8625– 8633. [PubMed: 21653866]

54. Stuphorn V, and Schall JD (2006). Executive control of countermanding saccades by the supplementary eye field. Nat. Neurosci 9.

55. Vlaev I (2011). Inconsistency in risk preferences: a psychophysical anomaly. Front. Psychol 2.

56. Tehovnik EJ, Sommer MA, Chou I-H, Slocum WM, and Schiller PH (2000). Eye fields in the frontal lobes of primates. Brain Res. Rev 32, 413–448. [PubMed: 10760550]

57. Payne BR, and Lomber SG (1999). A method to assess the functional impact of cerebral connections on target populations of neurons. J. Neurosci. Methods 86, 195– 208. [PubMed: 10065986]

58. Prelec D (1998). The probability weighting function. Econometrica, 497–527.

59. Burnham KP, and Anderson DR (2002). Model selection and multimodal inference (New York, NY: Springer).

60. Busemeyer JR, and Diederich A (2010). Cognitive Modeling (Thousand Oaks, CA: SAGE).

Author Manuscript

Author Manuscript

Author Manuscript

Author Manuscript

Highlights

- Monkeys show strong risk seeking during gambling.
- Medial frontal cortex (MFC) inactivation reduces the frequency of risky choices.
- MFC inactivation reduces the ability to suppress automatic, but maladaptive, responses to negative reward prediction errors.
- MFC inactivation does not affect adjustments of decisions based on reward history.

Author Manuscript

Author Manuscript

Author Manuscript

Author Manuscript

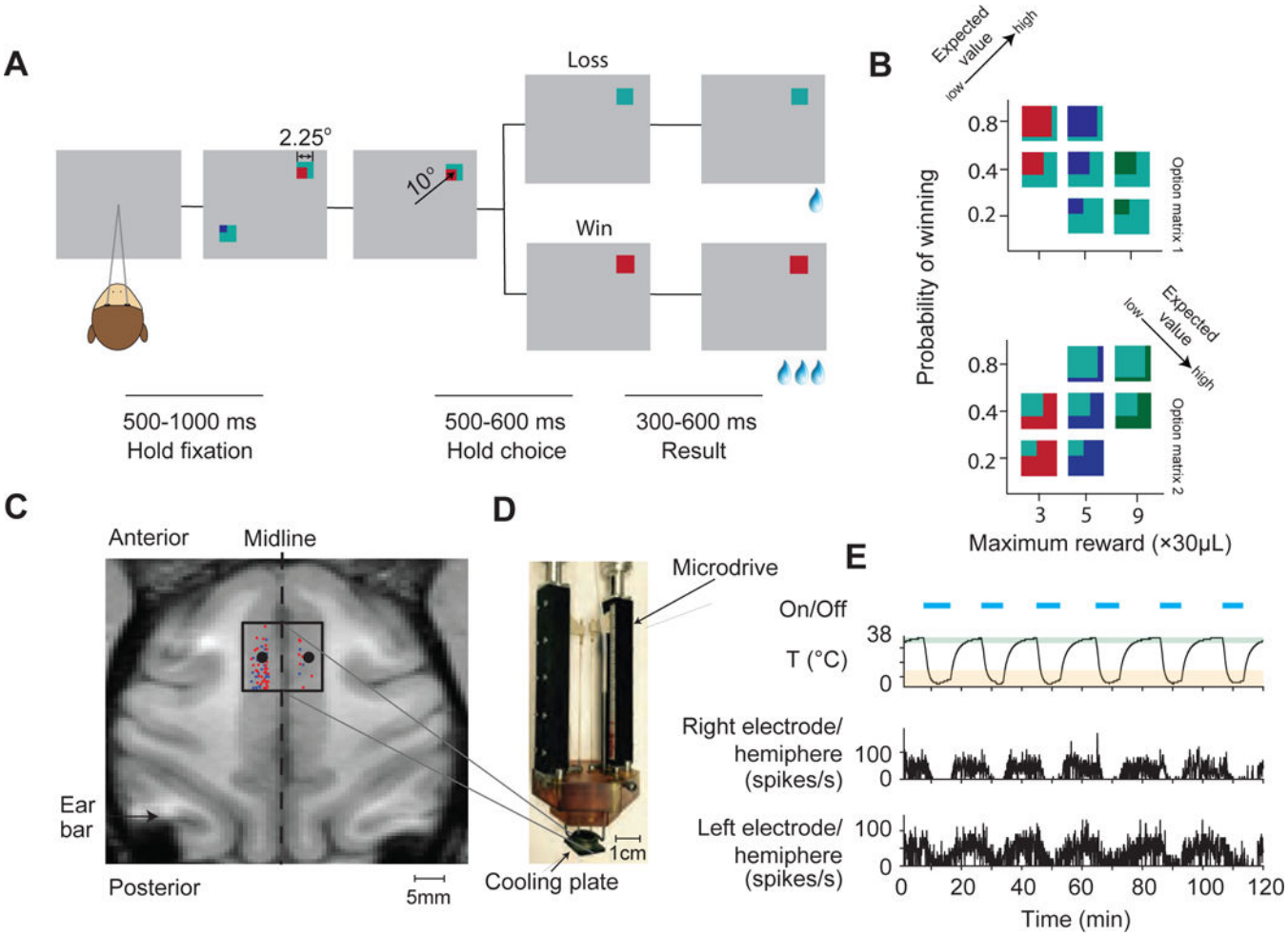

Figure 1. Task design and experimental setup.

(A) Task design and trial sequence. Monkeys fixated a white dot while two option stimuli were presented. Monkeys could earn a reward by making a saccade to one of the option stimuli. The lines below indicate the duration of epochs in the gambling task.

(B) Two sets of gamble options (option matrix 1 and option matrix 2) used in the gambling task. In a given session, we presented seven possible gamble options with three levels of maximum reward amount and three levels of winning probability (see Figure S1). Each option stimulus contains two colors. There are four different colors in total (cyan, red, blue and green) indicating four different reward amounts (increasing from 1, 3, 5 to 9 units of water, 1 unit = 30 μL of water). The proportions of the areas covered by the colors indicate the probability of receiving the corresponding reward. The expected value of the gamble targets increases along the axis indicated by the arrow (see Figure S2).

(C)Cryoinactivation experiment setup. The black square in the left subplot indicates the position of the cooling plate during bilateral inactivation. The black dots within the square indicate the recording sites at which neurophysiological recordings were performed during inactivation. Red dots indicate the recording sites where task related neuronal activity was recorded in separate experiments. Blue dots indicate the recording sites with no task related

Author Manuscript
Author Manuscript
Author Manuscript
Author Manuscript

neuronal activities. The back square indicates the cooling plate covers the majority of the cortical area with task related activity.

(D) The cooling device consist of three parts: the cooling plate (10 mm × 12 mm), the brown plastic cap, which stabilizes the whole cooling device in the recording chamber, and the two micro-drives, which hold two tungsten electrodes monitoring the neuronal activity during inactivation.

(E) A representative experimental session. The first row shows the on- and offset of the cooling device. The second row shows the temperature recorded at the cooling plate, right above the dura. The shaded green area indicates the temperature range defined as the control state, and the shaded orange area indicates the temperature range defined as the inactivation state. The third and fourth row shows the multi-unit spiking activities recorded simultaneously in both left (the third row) and right (the fourth row) SEF (see Figure S2).

Author Manuscript

Author Manuscript

Author Manuscript

Author Manuscript

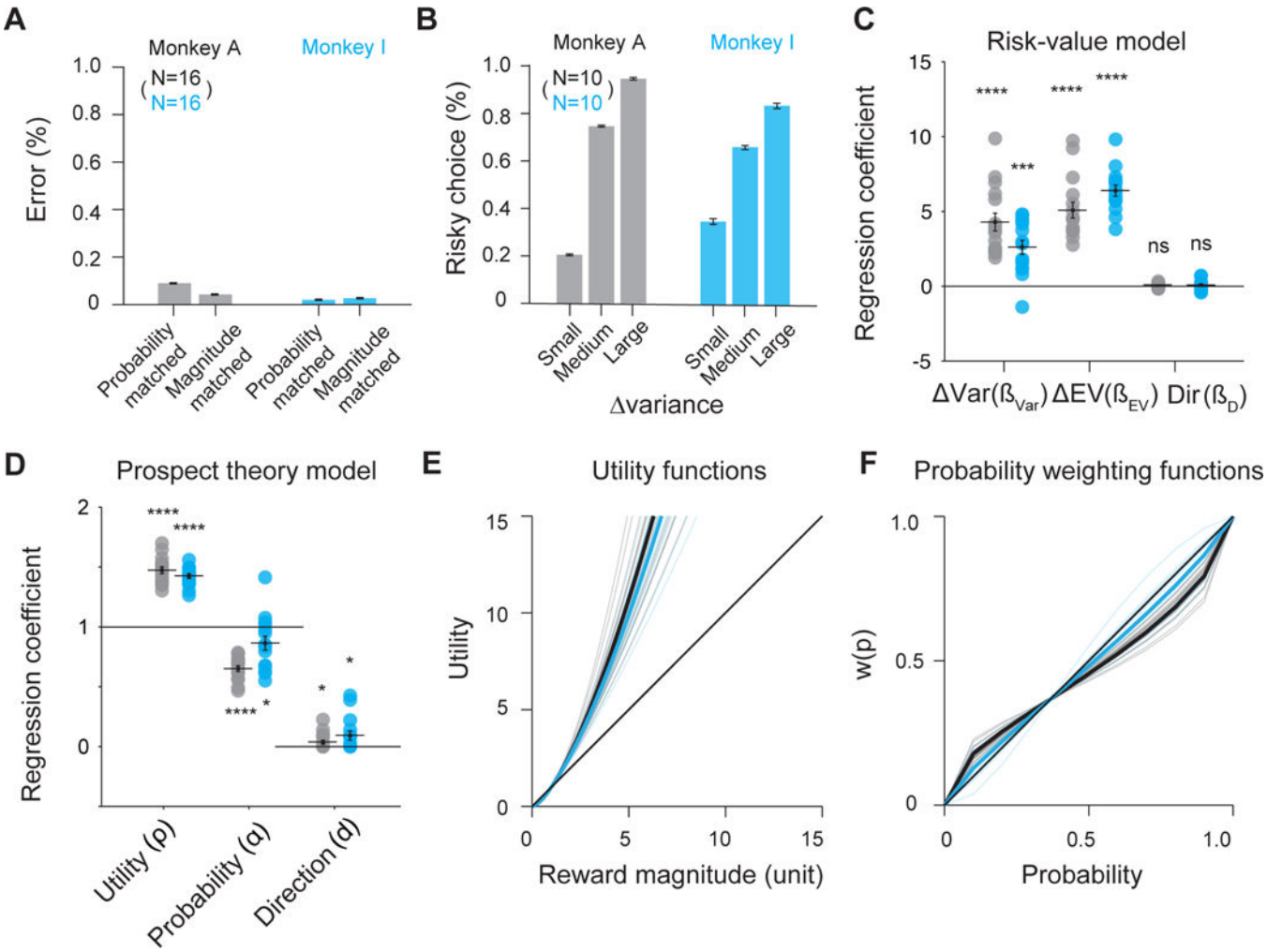

Figure 2. Monkeys show risk-seeking behavior.

(A) The monkeys showed first-order stochastic dominance. They strongly preferred the gamble option with the higher probability or higher amount, when the other factor (reward amount or probability) was held constant.

(B) The monkeys were risk-seeking. They strongly preferred the gamble option with higher variance, when expected value was identical for both gambles options. This preference increased with increasing variance differences.

(C) The risk-value model explains choices between two gamble options as a function of outcome variance differences (ΔVar), expected value differences (ΔEV), and directional bias (Dir). The regression coefficients for ΔVar and ΔEV for both monkeys are significantly different from 0 (t-test, $p < 10^{-4}$). (Monkey A: black; Monkey I: blue). The Var coefficients are positive, indicating attraction to risk. The regression coefficients for Dir are not significant different from 0. Each dot represents an estimated regression coefficient for one experimental session.

(D) The prospect theory model explains choices between two gamble options as a function of the non-linear utility of outcomes, weighted by a non-linear probability function, and the directional bias. The estimated coefficients for both utility and probability distortion are

Author Manuscript

Author Manuscript

Author Manuscript

Author Manuscript

significantly different from 1 (t-test, $p < 10^{-4}$). The estimated coefficients for direction is slightly above 0 (t-test, $p < 0.05$).

(E) The estimated power utility functions for both monkeys. The thin lines denote the individual session estimations, while the thick lines denote the average estimation. The utility functions are convex, indicating risk-seeking. (Monkey A: black; Monkey I: blue).

(F) probability weighting function using the 1-parameter Prelec weighting function for both monkeys. The color scheme is similar to f. Error bars denote s.e.m; *, p <0.05; ****, p $<10^{-4}$.

See also Figure S1 for choice patterns with both option matrices separately.

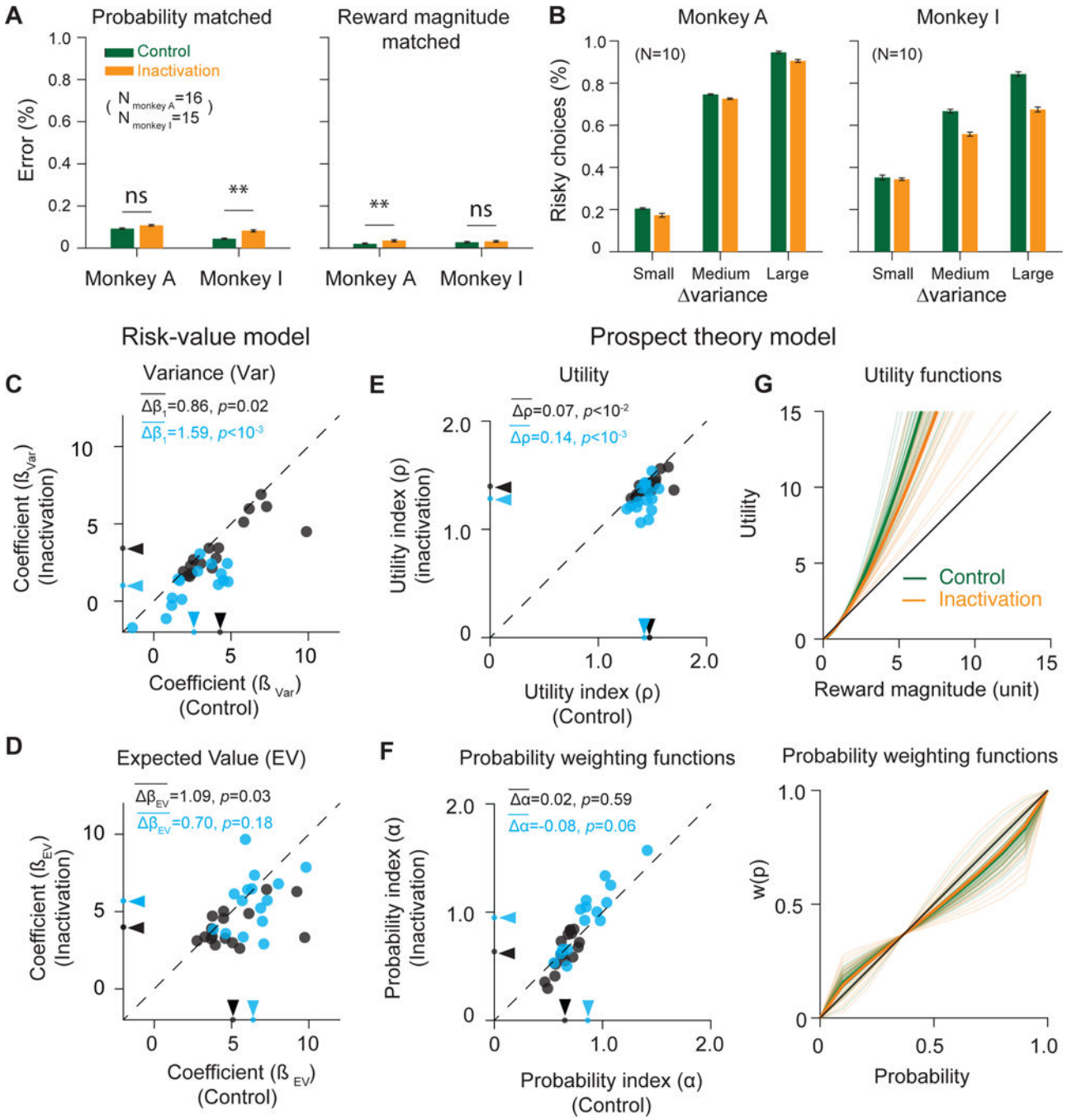

Figure 3. SEF inactivation reduces risk-seeking.

(A) Inactivation has only a small and non-consistent effect on the monkeys' ability to choose the optimal gamble option, if they vary only in one factor (either magnitude or probability). Error rates are low both in the control (green) and inactivation (orange) condition and do not show consistent differences across monkeys.

(B) Inactivation reduces risk-seeking. The preference for gamble options with larger outcome variance is less pronounced during inactivation (orange) compared to the control

Author Manuscript
Author Manuscript
Author Manuscript
Author Manuscript

Author Manuscript

Author Manuscript

Author Manuscript

Author Manuscript

(green) condition (paired t-test, Combined: p=1.46×10^{-3}; Monkey A: p=0.05; Monkey I: p=0.01).

(C–D) Reduction of risk-seeking estimated by the risk-value model.

(C) Comparison of the coefficients for risk (Var) in the control and inactivation condition for all experimental sessions (Monkey A: black; Monkey I: blue). The arrows indicate the mean value for each condition. The coefficients were consistently lower in the inactivation condition, indicating reduced preference for risk.

(D) The coefficients for expected value (EV) were slightly, but consistently decreased in the inactivation condition. All conventions are identical to C here and in all other scatter plots.

(E–G) Reduction of risk-seeking estimated by the prospect theory model.

(E) The parameter controlling curvature of the utility function is consistently decreased in the inactivation condition, which indicates reduced risk-seeking.

(F) The parameter controlling probability weighting is not significantly changed during inactivation.

(G) The corresponding utility functions (top) and probability weighing functions (bottom) are shown for both monkeys during the control (green) and inactivation (orange) condition. Thin lines indicate individual sessions, while thick lines indicate the average function. Error bars denote s.e.m.; paired t-test, ns, non-significant; *, p <0.05; **, p <10^{-2} ***, p <10^{-3}; ****, p <10^{-4}.

See SEF inactivation effect on saccade reaction times in Table S3. See reduction of risk-seeking estimated by the prospect theory model separately for both monkeys in Figure S4C.

Author Manuscript

Author Manuscript

Author Manuscript

Author Manuscript

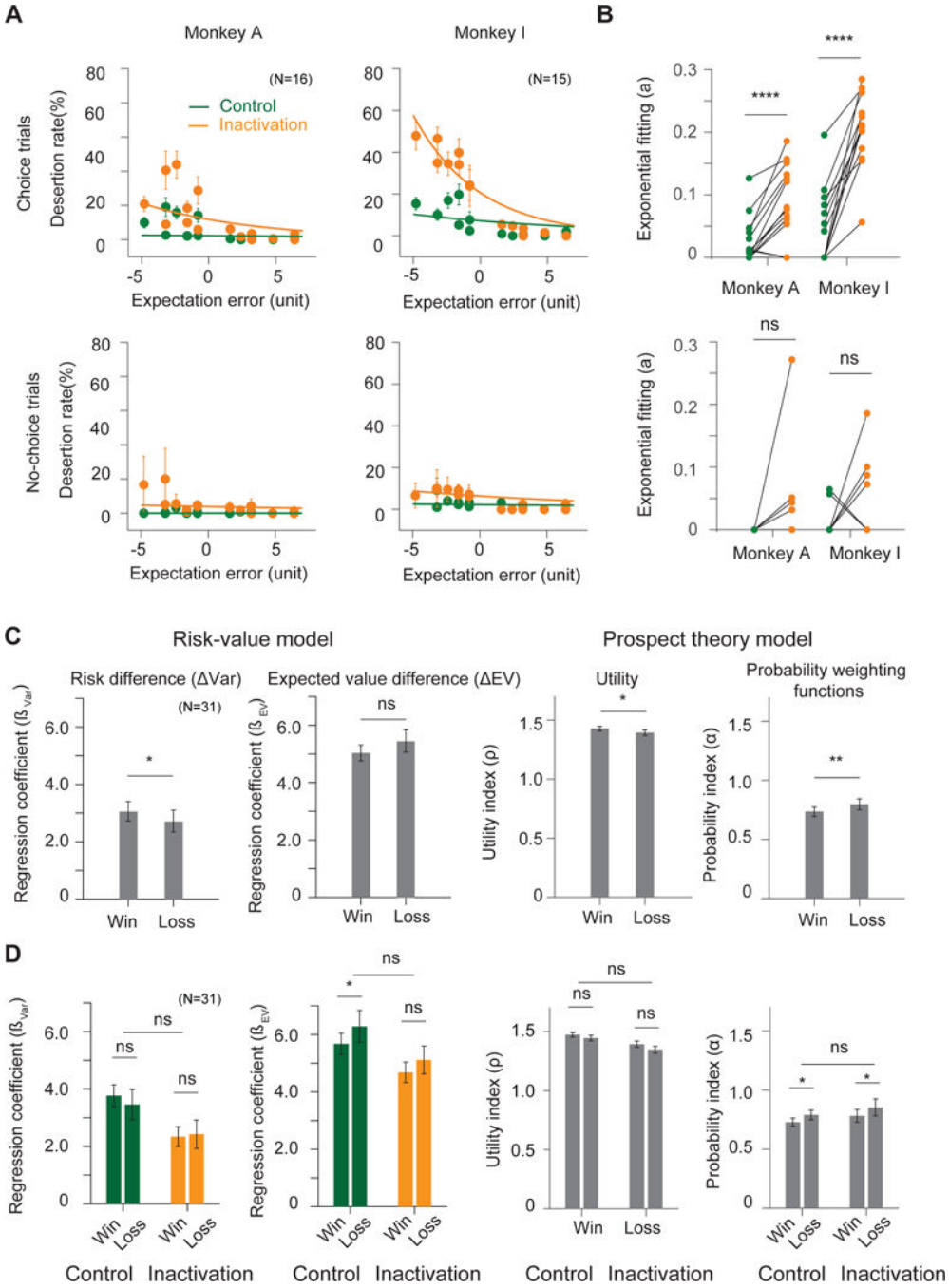

Figure 4. Influence of SEF inactivation on desertion rates and gamble history effect.

(A) Desertion rates during result periods as a function of reward expectation errors, the differences between actual and anticipated reward, during control (green) and inactivation (orange) condition in choice trials (top) and no-choice trials (bottom). The overall desertion rates are estimated using an exponential fit, indicated by the colored lines. These rates are significantly increased during inactivation in choice trials. This increase is larger with larger negative prediction errors. Trial desertion here is defined as making saccades actively

Author Manuscript

Author Manuscript

Author Manuscript

Author Manuscript

outside of the fixation windows (see Figure S3C and D). See Figure S4 for trial quitting rates in other task epochs.

(B) Changes of scaling parameters of the exponential functions for each individual experiment session in choice trials (top) and no-choice trials (bottom). Each line shows the change in the scaling parameters in control and inactivation condition from one experiment session.

(C) Changes of risk preference based on gamble outcome history across trials during both control and inactivation conditions. The monkeys were less risk-seeking following a lost gamble as compared to a won gamble. This effect is captured both by the risk-value (left two plots) and the prospect theory (right two plots) models. In the risk-value model, the risk coefficient is significantly lower on trials following a gamble loss, while the expected value coefficient stays the same. In the prospect theory model, the utility function becomes less concave (ρ closer to 1) and the probability weighting function becomes more linear (α closer to 1) on trials following a gamble loss.

(D) The effect on risk preference by gamble outcome history does not change across control (green) and inactivation (orange) conditions. Error bars denote s.e.m.; paired t-test, ns, non-significant; *, $p < 0.05$; **, $p < 10^{-2}$ ***, $p < 10^{-3}$, ****, $p < 10^{-4}$.